

# **Plug-In Hybrid Electric Vehicle Charger System**

## **Senior Project Final Report**

**By: Matthew Daly, Peter Burrmann & Renee Kohl**

**Advisors: Dr. Woonki Na & Dr. Brian Huggins**

**May 9<sup>th</sup> 2012**

## Table of Contents

Abstract .....	3
Introduction .....	4
Project Description.....	4
Theory .....	5
High Power System .....	5
AC/DC Diode Rectifier .....	6
Bi-Directional Converter .....	6
Boost Converter and Power Factor Correction.....	7
Buck Converter.....	8
Low Power/Interfacing System.....	9
Current Transducer .....	11
Gate Driver .....	11
Li-Ion Battery.....	13
Internal Resistance.....	15
Software/Controller.....	16
Bi-directional Converter.....	21
Completed Work.....	27
Future Work.....	27
IMPLEMENTATION AND SIMULATION .....	27
Experimental/Simulation Setup, Results and Discussion.....	28
Power factor Correction.....	28
Bi-Directional Converter (Buck and Boost) .....	29
Overall Schematic .....	33
Conclusion.....	34

## Abstract

A Plug-in Hybrid Electric Vehicle (PHEV) is not only a hybrid vehicle which utilizes a battery to power the vehicle's electric motor, but also its battery can be recharged when it is plugged-in to a power source (typically 120V<sub>rms</sub>) from the grid. PHEVs have much higher fuel efficiency and lower operating cost than the conventional internal combustion engine based vehicle. These electric vehicles help keep the environment clean by reducing the amount of toxins emitted from standard exhaust systems. The primary goal of this project was to design a charging and discharging system for the PHEVs vehicles through the use of Digital Signal Processor(DSP) based power electronics systems. In this report, the progress toward this goal is addressed with using a 400W, 51.8V Li-Ion batteries and a Texas Instrument 32-bit fixed-point DSP TMS320F2812.

## **Introduction**

Lately, the hybrid drivetrain technology has drawn attention of the both media and automobile consumers because vehicles employing the hybrid technology can significantly improve their fuel economy and produce less pollutants compared to conventional vehicles. For further seeking a better hybrid electric vehicle(HEV) technology, the plug-in-hybrid electrical vehicle(PHEV) emerges by incorporating this hybrid technology with adding the function of plug-in-charging from the utility grid. For a PHEV, it needs a larger motor, more energy storages such as batteries or ultracapacitors and less space for engine and gas tank comparing with the normal hybrid vehicle.

## **Project Description**

The primary goal of this project is to design a system that will function as an electric vehicle charger. A Digital Signal Processor (DSP) driven power electronics system shall be designed such that the system can convert 120V, rms AC grid power to the required 51.8V, peak DC value to charge an electric vehicle battery. This system will consist of a single phase diode rectifier, boost converter, and bi-directional converter for discharging the battery into a variable load or charging of the battery itself. In order to implement this system, a control algorithm is to be developed using the TMS320F2812 DSP board. Values for all circuit elements need to be calculated and specific devices and circuit elements need to be selected and purchased to meet the system specifications.

## Theory

The design of an onboard battery charger is not as simple as connecting the battery straight to the grid. The power charging the battery must be within certain specifications to prevent damage to the battery and overall system. In terms of PHEVs, the high- energy battery pack is to be charged with Power Factor Correction(PFC) from an AC outlet. The most common topology for the PHEV battery charger is the two-stage approach with cascaded PFC AC-DC and DC-DC converters. In the PFC stage, AC single phase is rectified and boosted with power factor correction. The output of the boost converter is connected to the DC bus, and a bidirectional converter for the battery charging or discharging is also connected to this DC bus.

## High Power System

The high power system is responsible for handling the high voltage and current of the overall system. It contains multiple systems including a Diode rectifier, Boost converter and Bi-directional converter. The best way to design the high power system is in a modular approach. This means that each part is designed separately and then combined together to make the overall system. Figure 1 shows the system topology.

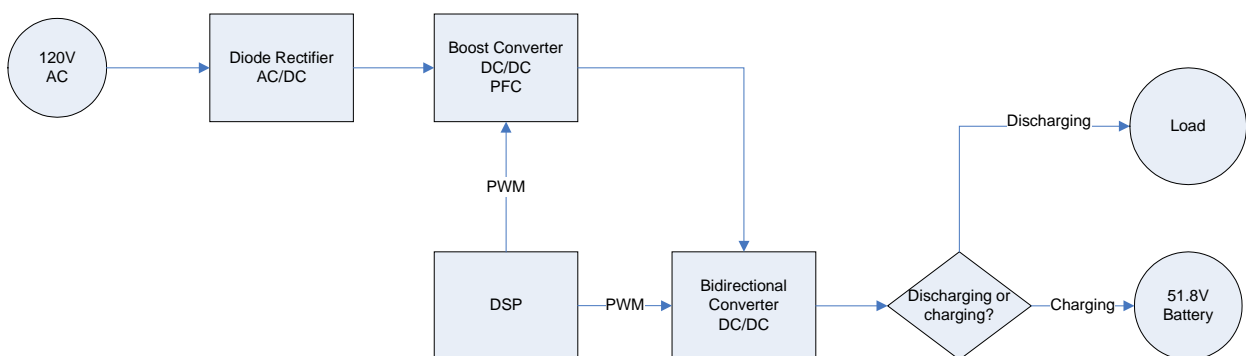


Figure 1 System Block Diagram

### AC/DC Diode Rectifier

The diode rectifier is responsible for taking in the sinusoidal AC main voltage and converting to a DC voltage. If the designer chooses to have a controlled output voltage, IGBTs, or thyristors are used as an AC to DC switch-mode rectifier, otherwise an uncontrolled rectifier will just use diodes[1]. For the design of the Plug-In Hybrid Electric Vehicle Charger an uncontrolled diode rectifier is what will be used in Figure 2.

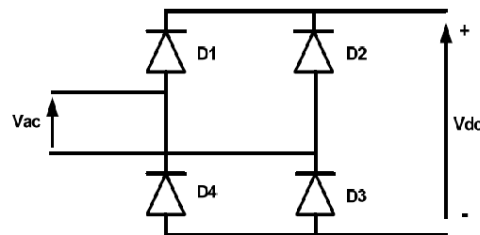


Figure 2 Uncontrolled Diode Rectifier [1]

When the input voltage is positive, diodes D1 and D3 are conducting because these diodes are forward biased. At this time diodes D2 and D4 are in “off” states. On the contrary, when the input voltage is negative, D2 and D4 are conducting, and D1 and D3 are in “off”[1]. As described, the switching functionality of the diodes converts a sinusoidal wave into a positive rectified sinusoidal waveform.

### Bi-Directional Converter

The purpose of the Bi-Directional converter in the PHEV charger system is to interface the battery with the system enabling it to charge and discharge when needed. In a buck mode, this converter will lower the output voltage going to the input of the battery to a safe level enabling the battery to safely charge to a full level. When the system is not charging, the converter can be switched into its second mode. In this mode, the battery will discharge and increase (boost) the voltage to the level desired to drive the load. The Bi-Directional converter is shown in Figure 3.

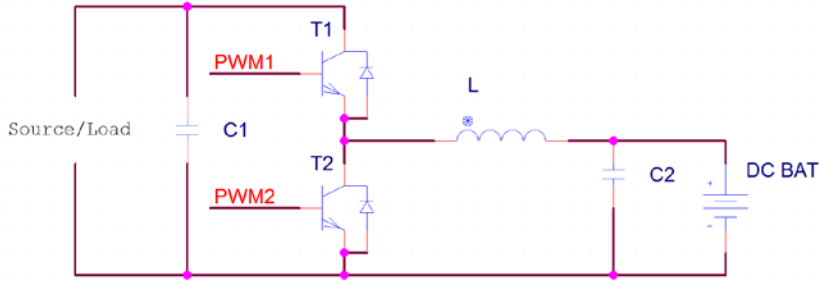


Figure 3 Bi-Directional Converter [2]

The bi-directional functionality of this circuit is given by the two switching transistors, T1 and T2. These transistors will receive complementary control signals from the DSP directing the flow of current. When the current through the inductor, L, is positive, the converter will be in buck mode. When the current through the inductor is negative the converter will be in boost mode [3].

### Boost Converter and Power Factor Correction

Power factor correction will be implemented to greatly improve the efficiency of our system. Power factor is defined as a ratio between real power and apparent power [2]. Real power is the actual amount of power being used, or dissipated, Apparent power is the combination of real power and reactive power. Because of this reactive power from reactive loads such as inductors and capacitors, the PHEV charger system consumes wasted power which lowers efficiency of the system. Thus unity power factor is desirable. Through our power factor correction system we will increase the amount of real power and reduce reactive power. This goal can be achieved through the use of a switch- mode boost converter, as shown in Figure 4.

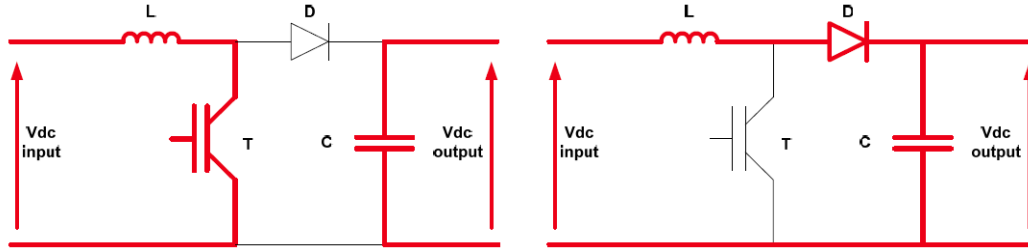


Figure 4 The 2 stages of the Boost Converter used for PFC [1]

According to Figure 4, we can see how the Boost Converter works. In the PHEV system we will essentially be using two boost converters to achieve two different goals. As previously stated a boost converter will be used for power factor correction. The transistor will alter its duty cycle to align the voltage and current waves. This process will be covered later in the DSP controller portion. The second use of the boost converter is part of the bi-directional converter for boost mode. It will be responsible for discharging the battery and raising the voltage to a level suitable to power a load. In Figure 4 the circuit on the left, the transistor T, is turned on and the diode D, is turned off, in this stage, the energy is stored through the inductor. In the circuit on the right, the stored energy in the inductor is transferred to the load. It is understood that the output voltage is dependent on the rate of change of its current. This provides steady power through the load and into the capacitor. When the system switches back to the previous stage, the capacitor's energy storage characteristic continues to produce a steady output. The capacitor is also responsible for reducing ripple in the output signal. The output voltage, inductor value, and capacitor value can be calculated with equations (1-3)

$$V_{out} = \frac{1}{(1 - \alpha)} V_{in} \quad (1) \quad L = \frac{V_{out}}{4 f_{swi \ max} \Delta I} \quad (2) \quad C = \frac{V_M I_M}{2 \Delta V_{out} \omega V_{out}} \quad (3)$$

### Buck Converter

The buck converter makes up the second half of the bi-directional converter. The purpose of the buck converter as previously stated is to lower the DC link voltage to a voltage



suitable to charge the DC battery. If too much voltage were to go into the battery it would be destroyed.

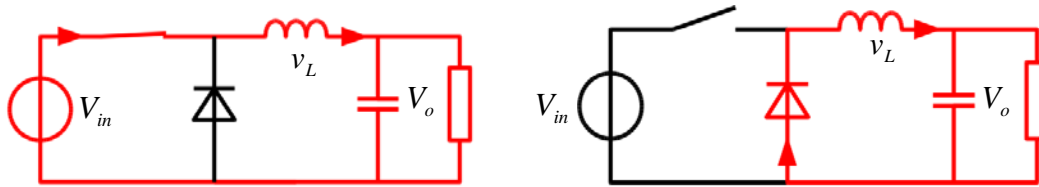


Figure 5 the two stages of the buck converter

In Figure 5 the circuit on the left, the transistor is closed, and the voltage across the inductor is  $v_L = V_{in} - V_o$  and the current through the inductor will rise in a linear fashion. In this stage the diode is reverse biased. Once the transistor is switched open on the circuit on the right, the diode goes forward biased and the voltage across the inductor is  $v_L = -V_o$  and the current of the inductor decreases. The equations for calculating the effects of the buck converter are below equation 4.

$$V_o = \alpha V_{in} \quad (4)$$

Where  $\alpha$  is the duty ratio of the buck converter.

### Low Power/Interfacing System

The low power system is responsible for interfacing the Digital Signal Processor (DSP) with the high power system. This includes taking voltage and current measurements from the high power system to determine how to control the switching transistors. Also, the low power system includes the gate drivers responsible for relaying output signals from the DSP to the transistors. This set of important circuitry could be best described as the bridge between the body and brains of the overall system.

## Voltage Sensor

The voltage sensor circuit will be used to take the voltage level readings and send them to the DSP. The reason we cannot directly connect the DSP to the high power circuitry is because the maximum input value to the DSP's I/O ports is 3.3V. In order to sense the voltage, we will have to scale the voltage to a value between 0 and 3.3V to represent the higher voltage. This can be done with the use of a voltage divider circuit, op-amp in a unity gain buffer configuration and two schottky diodes for the protection from the high power circuits. This circuit is shown in Figure 6.

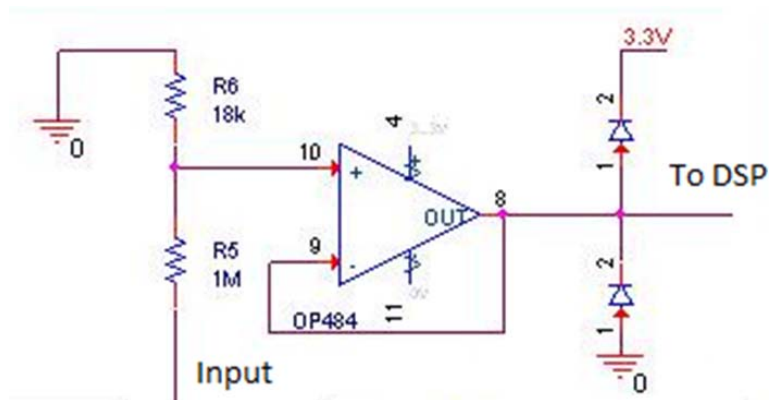


Figure 6 Voltage Divider, Op-Amp and Diode protection circuit

Each sensor input is the desired area of measurement on the high power circuit. The voltage divider input/output equation is shown below in equation 5.  $V_{in}$  will be the highest expected voltage from the high power circuit and  $R1$  and  $R2$  can be selected to produce a max  $V_{out}$  of 3.3V.

$$V_{out} = \frac{R2}{R1 + R2} \cdot V_{in} \quad (5)$$

The op-amp used after the voltage divider will be used as a unity gain buffer. The op-amp will receive a supply voltage of 0 and 3.3V. An Op-Amp's positive and negative input terminals have a very high impedance this will protect the DSP for current spikes that could

destroy the DSP. The reason we use the Op-Amp in a unity gain buffer configuration is to utilize the high impedance feature while keeping the voltage the same as the input. Lastly there are two schottky diodes, one connected from the output to 3.3V and the other is connected from ground to the output. In the case of a voltage that goes above 3.3V or below 0 volts into the negative range the diodes will pull the voltage to 0 or 3.3V, protecting the delicate hardware of the DSP.

### **Current Transducer**

A current transducer will be used to detect current values in the high power circuit. These values will be sent to the DSP to control the switching of the transistors in the high power sub-systems. The current transducer uses the Hall Effect to represent the current value as a voltage. The output voltage of our current transducers is 4V and unfortunately cannot be fed directly into the DSP. In order to work around this we implemented the voltage sensor circuit and adjusted the voltage divider to handle an input of 4 and output 0V to 3.3V.

### **Gate Driver**

The gate drivers are used as a medium between the pulse-width modulated output of the DSP and the input to the switching transistors of the high power circuit. Gate drivers are needed because the DSP's PWM output does not supply a high enough voltage to physically switch the transistor. The gate driver has its own power supply and simulates the DSP's output at a higher power level to effectively control the switching characteristic of the transistor. The IRFP460A high power MOSFET used in this system requires a gate-to-source voltage of approximately 12V to completely turn on. Since the DSP provides an output PWM of approximately 3.3V at low current, the gate driver would need to provide extra power to the signal to fully turn on the MOSFETs. For the MOSFETs involved in this system, the IR2110 gate driver was selected. The IR2110 is operational for high voltage applications (up to 600V). Figure 7 shows a typical

configuration for the IR2110 connected to a half bridge. This is also the setup used for driving the Buck converter gate and the PFC gate. The two output ports LO and HO on the IR2110 are independent of each other and driven by LIN and HIN respectively.

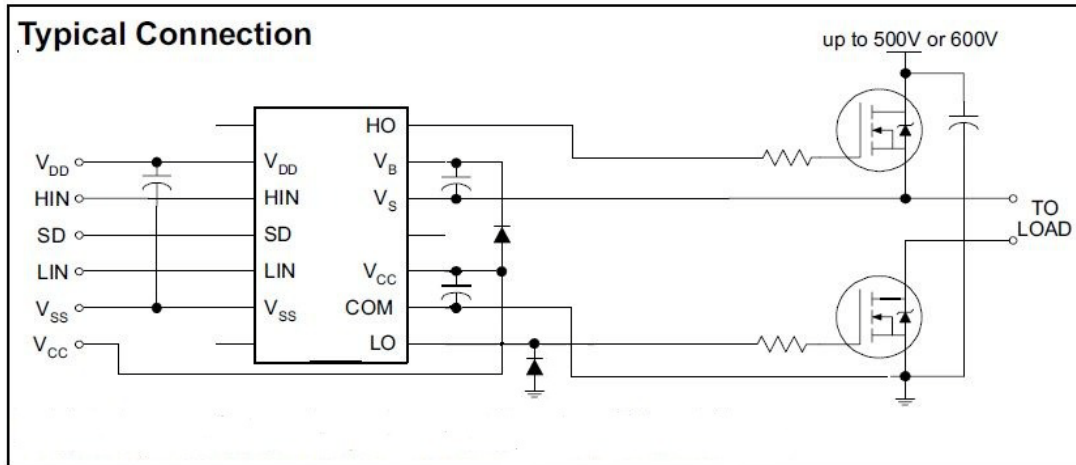


Figure 7 Typical Gate Driver configuration of IR2110

The LO output applies the voltage value of  $V_{cc}$  to the LO side MOSFET gate. The HO output provides enough voltage to the high side MOSFET gate such that the gate-to-source voltage maintains a drop of at least 12V. This is accomplished via the bootstrap capacitor that is shown in Figure 7 between  $V_B$  and  $V_S$ . The calculation for the bootstrap capacitor is shown below in equation(6) where the definitions of each of the variables are explained in application notes for the IR2110[7]. Once the correct value of the capacitor is calculated, it is recommended in practice to multiply that value by an order of magnitude in order to maintain a safety cushion.

$$C \geq \frac{2 \left[ 2Q_g + \frac{I_{qbs(max)}}{f} + Q_{Ls} + \frac{I_{Cbs(leak)}}{f} \right]}{V_{cc} - V_f - V_{LS} - V_{Min}} \quad (6)$$

This bootstrap capacitor is necessary for the Buck converter because the source of the MOSFET in the Buck converter is not tied to a high power ground. This causes the source voltage to be non-zero and requires a higher voltage than the value of  $V_{cc}$  alone. Note that the

frequency of operation plays an important role in what size this capacitor may be. As the high side MOSFET turns off, current flows from  $V_{cc}$  through a diode into  $V_B$ , and thereby charging the bootstrap capacitor. Once the High side MOSFET needs to turn on, charge is pulled from the capacitor and  $V_{cc}$  in order to produce the necessary increase in voltage for properly switching the MOSFET.

## Li-Ion Battery

One of the primary goals of this project is to optimally charge a high power battery. The battery selected for charging is a 14 Cell (58.8V) Lithium-Ion Polymer Battery with a total rated capacity of 10[Ah] and can be seen in Figure 8.



Figure 8 58.8[V] Lithium Ion battery pack

In order to optimally charge a Li-Ion battery, an understanding of various charging methods and charging stages of Li-Ion cells is necessary. A break-down of the charging stages can be seen in Figure 9. Note that the plot applies to a single Lithium cell.

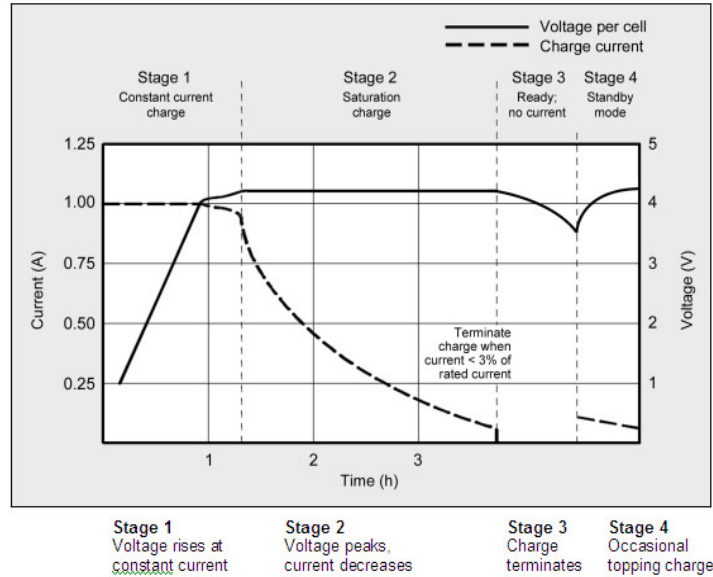


Figure 9 Charging Stages of a Lithium Polymer Battery[5]

Each lithium-Ion cells has a potential of 4.2V at maximum capacity. As the battery discharges, the operating voltage drops in kind. However, there is a state of charge where the battery is at maximum voltage, but is not fully charged. As seen in Figure 9, the first stage of charging is constant current charging. This is where a variable voltage is applied the battery to maintain a constant current flow until the battery reaches its maximum rated voltage (in our case, 58.8V. At that point, the voltage is kept constant, and the current applied is gradually reduced over time until the battery is on being charged at 3% of its rated current value (in our case, 300mA). This second stage of charge is known as the saturation stage where the charge on the surfaces of the anodes and cathodes are dispersed throughout the bodies of the cells. Stage 3 simply represents the point when the battery is ready to operate as expected. Stage 4 briefly describes the situation of what the battery does when it is idle for quite some time.

During standby mode in stage 4, the battery gradually and slowly leaks charge. The self discharge associated with some batteries is often countered with a process known as trickle charging. Trickle charging is the process of applying small pulses of charge to the battery at a

rate equal to the self discharge of the battery. While this sounds good on paper, this is a poor plan for Li-Ion batteries. Maintaining maximum state of charge on a Li-Ion battery puts a large amount of stress on the cells, and shortens the overall lifespan of the battery. Maintaining maximum charge or even potential over-charge causes metallic lithium plating on the cell nodes. The plating causes poor power transfer during charging and discharging and ends up dissipating large amounts of energy into heat.

### Internal Resistance

In order to maintain a constant current being applied to the battery, we need to know the internal resistance of the battery. To assist with this, a battery model can be developed for the Li-Ion battery. A generic model can be seen below in Figure 10.

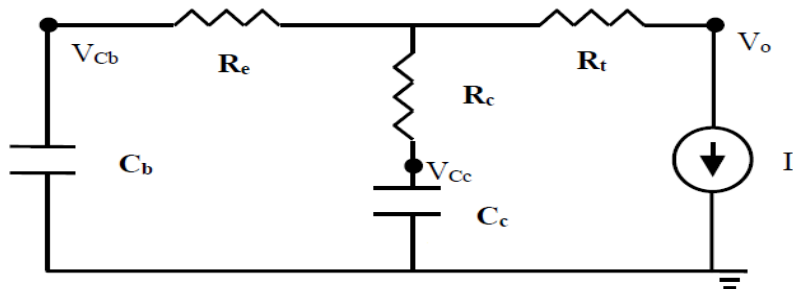


Figure 10 Generic Lithium-Ion Battery Model[6]

The problem encountered with the model in Figure 10 is that finding the individual components for the battery model is almost impossible without some form of software taking multiple data points as the battery runs through several discharge cycles. The reason such a detailed process is required is that the internal resistance values vary slightly with State of Charge, temperature of the battery, and rate of charge/discharge. To demonstrate the concept on how we would take measurements of the battery's internal resistance as a whole, a single pulse discharge was applied over period. Of approximately 30 seconds in Figure 11.

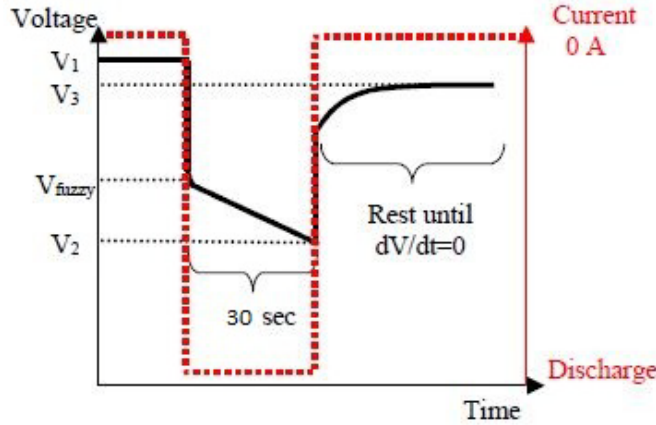


Figure 11 Singular Pulse discharge of a Battery with relevant measurements[6]

From this process, we were able to derive a single value for the overall internal resistance of our battery at approximately 90% SOC. The data taken is in table 1. We were able to find out that the internal resistance of our battery when at high capacity is 108mΩ. This tells us only what the overall resistance is at that state of charge. A more complete table would need to be formed in order to have an accurate model for the battery. With an accurate model, we would be able to control the voltage applied to the battery via controller much great precision.

Table 1 – Voltage measurements for Li-Ion battery after 30 second pulse discharge

Vr	56.530
R	10.910
V1	57.850
V2	57.160
V3	57.720
I	5.181
Rint	0.108

## Software/Controller

The brains of the PHEV charger system is the digital signal processor or DSP. “A Digital Signal Processor is a super-fast chip computer, which has been optimized for the detection, processing, and generation of real world signals such as voice, video, music, etc, in real



time.”[5]. This fast, high precision processor is ideal for controlling the overall converter system. The DSP is programmed with C code. C code can be written or generated with a block diagram model via Matlab Simulink toolboxes. As previously noted, the DSP can generate a pulse width modulated signal which is fed to the gate drivers powering the switching transistors. Pulse width modulation, or PWM, is generally a square wave signal with a constant frequency; the duty cycle is then adjusted [4]. This adjustment of the duty cycle is what determines the on and off time of the switching transistors. For the PHEV charger system, dead-band will have to be incorporated into the PWM signal to prevent switching crossover. “Dead-band separates the transition edges of two signals: output and complemented output, by a time interval.”[4] The purpose of dead-band is to protect the sensitive hardware on the high power side. If two complementary transistors are on at the same time, damage and instability of the power circuits will occur.

In order to determine the duty cycle of the PWM signal, calculations must be performed. The voltage and current values from the low power circuitry are fed into the DSP’s analog to digital converter. The DSP will take these input values and apply them to control algorithms. This will generate a change in the duty cycle of the PWM signal. The on and off times are always changing in order to generate a desired output in multiple areas of the high power circuit.

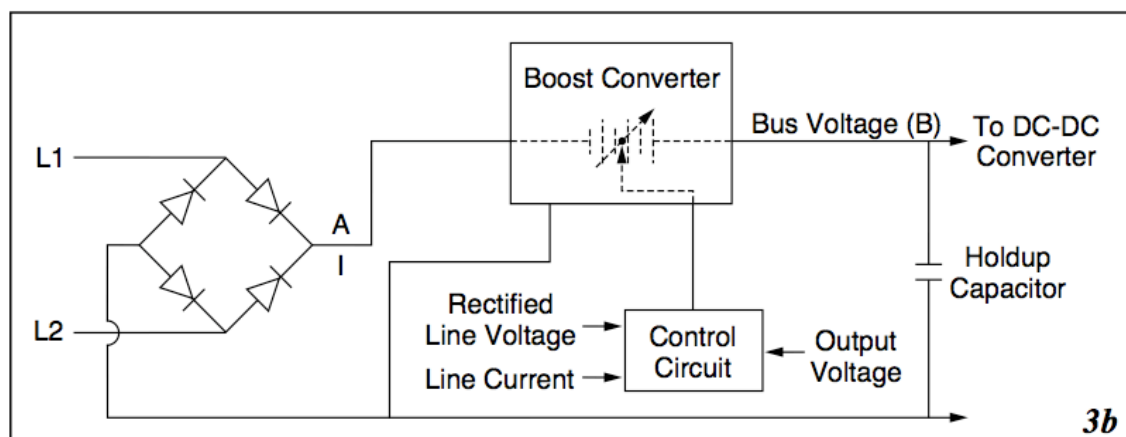


Figure 12 Power Factor Correction Boost Converter Circuit

As seen in Figure 12, the PFC circuit is controlled by the DSP. The DSP reads in the rectified sine wave input, the current through the inductor, and the output voltage. As mentioned earlier we are using this active power factor correction method in attempt to achieve a unity power factor. The way this boost converter circuit accomplishes that is by comparing the output voltage to a constant reference. This reference value is the target output voltage that we choose. The error then passes through a PI controller and then multiplied by the rectified sine wave to create a reference current. From there the current is compared to the reference that was created and that error passes through a second PI controller. The output is then the duty cycle that is sent to the MOSFET.

After building the PFC circuit we applied a 50% duty cycle from an open loop control and you can see in Figure 13 the current in channel 2 has a large ripple. With a PI controller the ripple will be reduced to create a clean current and a unity power factor. Channel 1 shows the output of the current sensor that inputs into the DSP.

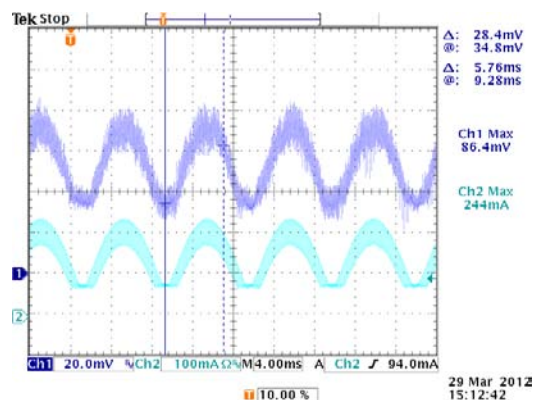


Figure 13 Open loop control, 50% duty cycle

Notes: Channel 1: output of current sensing circuitry and op amp input to the DSP  
 Channel 2: output of current probe (expected to be noisy because no PFC is implemented)

The 80mV out of the op amp can be converted by multiplying by the 1.25 voltage divider, then multiply by 50/4 for the current sensor, and divide by 5 to factor in the 5 loops around the current sensor gives you 250mV which the current probe is showing.

To test the hysteresis control of the current we applied the control you see in Figure 14. We simulated a current reference using a sine wave generator and an absolute value in Simulink. After the actual current is read in through the ADC converter it is compared to the reference value and if the reference is greater the pwm is high and vice versa. The current that previously looked like channel 2 in (a) of Figure 13 was smoothed out to the current that appears on channel 2 in Figure 15.

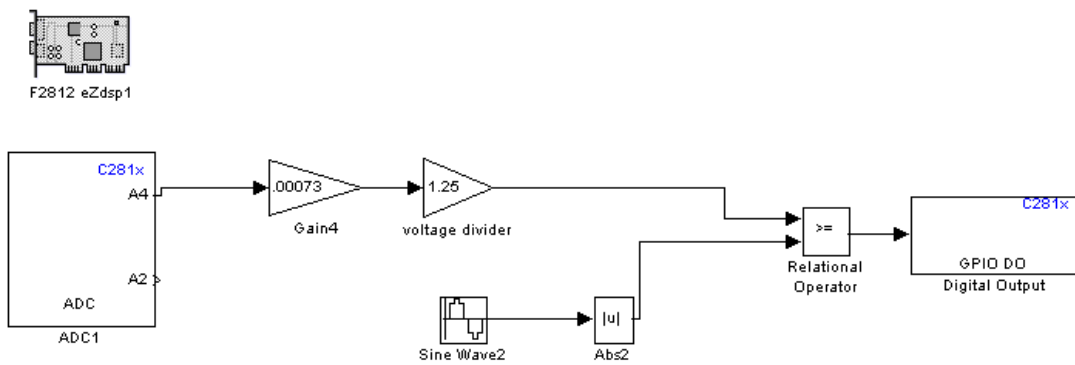


Figure 14 Simulink hysteresis control

Because the current being measured by the DSP is a rectified sign wave with an amplitude of approximately 80mV we simulated this in Simulink as the reference current to match.

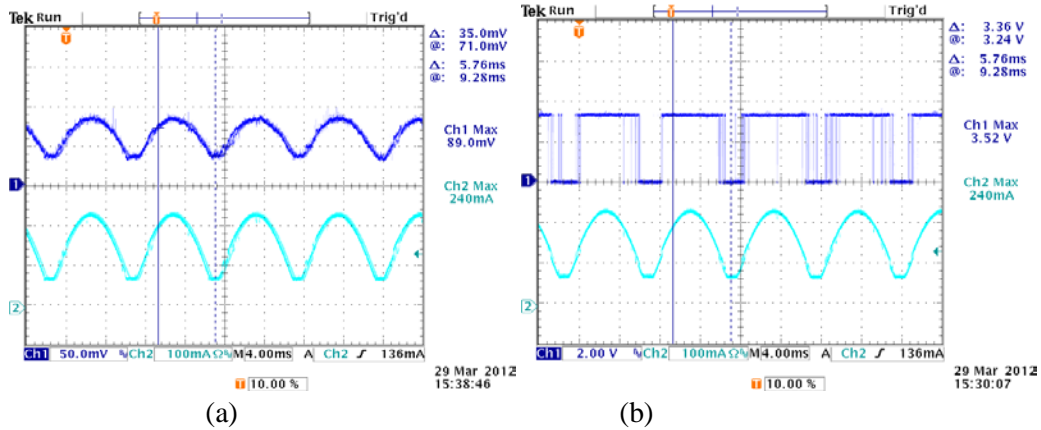


Figure 15

Channel 1: output of protection circuitry Channel: constantly adjusting PWM  
 Channel 2: current through inductor

When testing the PFC controls, the signal generator used to create the sine wave would reach the current limit and lower the output voltage to an unusable value. In order to lower the current we increased the size of the load resistance to 10kΩ. This allowed the signal generator to output the full 10V<sub>PP</sub> sine wave, but this caused the circuit to go into discontinuous mode as seen in Figure 17 on channel 1. Even in discontinuous mode, the voltage could be controlled by changing the constant voltage reference in code composer when the control system in Figure 16 was applied.

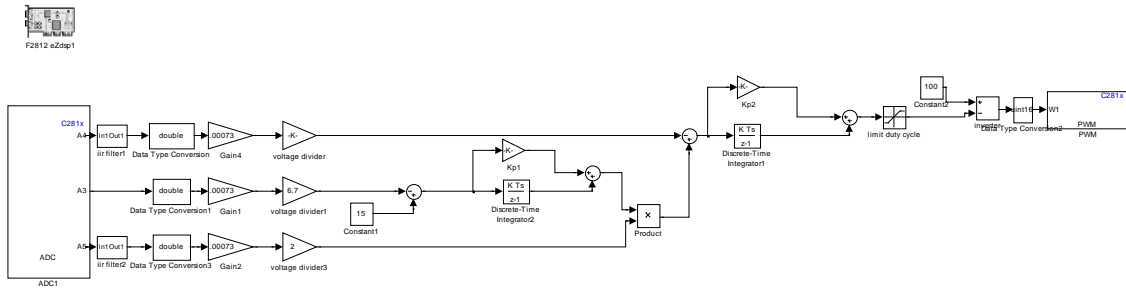


Figure 16 Simulink control system for PFC circuit

As you can see in Figures (a)-(c) in Figure 1,8 the output voltage of the PFC is very accurate when compared to the reference voltage entered.

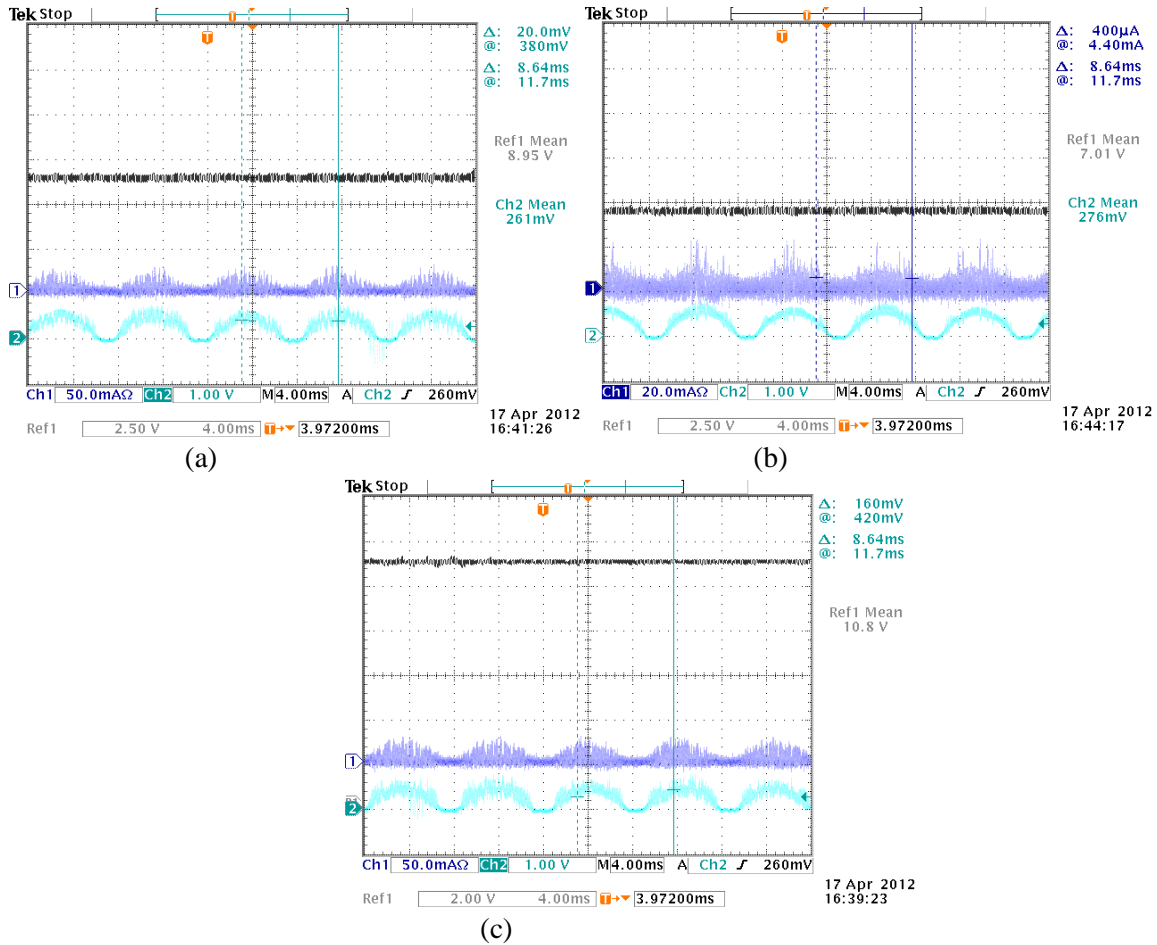


Figure 17

Notes: Channel 1 shows current through inductor  
 Channel 2 shows input voltage  
 Reference shows the output voltage. Reference values: (A) – 9V, (B) – 7V, (C) – 11V.

### Bi-directional Converter

Because the bi-directional converter acts as a buck converter as the current flows towards the battery and as a boost converter as the current flows out of the battery we can use separate controls for each of these modes. Then by comparing the voltages being read in and using logic we can determine whether we have to be using the boost controller or the buck controller. Using equation (7) we found the transfer function for our small scale buck converter to be:

$$\frac{4.04 \times 10^7 + S \cdot 6060.6}{S + S \cdot 309.7 + 2.02 \times 10^7} \quad (7)$$

Using the Matlab code in Appendix A, we generated bode plots for the magnitude and phase of the power stage of the buck converter as seen in Figure 18.

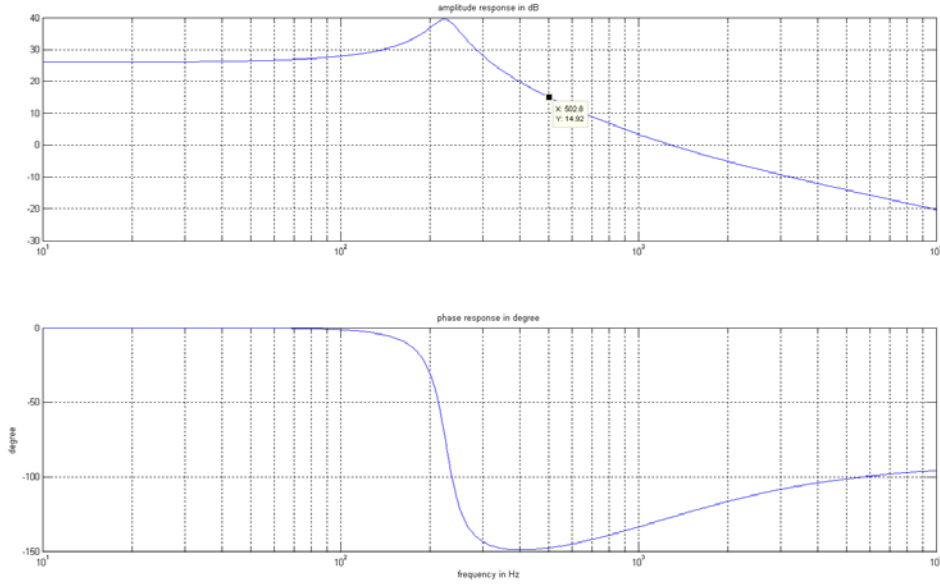


Figure 18 Phase and Magnitude plots for power stage Phase and Magnitude plots for power stage

From Figure 18 we can choose a crossover frequency,  $f_c$ . As  $f_c > \frac{1}{2\pi\sqrt{LC}}$  we chose  $f_c$

=500Hz. Therefore,  $|G_{ps}(s)|_{f_c} = 15.12dB$  or 5.7, and  $\angle G_{ps}(s)_{f_c} = -150^\circ$ .

The transfer function of our PI control block is:

$$G_c(s) = \frac{sk_p + k_i}{s} \quad (8)$$

So the magnitude can be found by

$$|G_c(s)|_{f_c} = \sqrt{k_p^2 + \left(\frac{k_i}{\omega}\right)^2} \quad (9)$$

and phase

$$\angle G_c(s)_{f_c} = \tan^{-1} \left( \frac{-\frac{k_i}{\omega}}{k_p} \right) \quad (10)$$

In order to find the magnitude of the controller at our crossover frequency we use:

$$1 = |G_c(s)|_{f_c} \cdot |G_{pwm}(s)|_{f_c} \cdot |G_{ps}(s)|_{f_c} \cdot k_{fb} \quad (11)$$

or

$$1 = |G_c(s)|_{f_c} \cdot .263 \cdot 5.7 \cdot 1$$

$$|G_c(s)|_{f_c} = .667$$

We set the phase margin to be:

$$\phi_{pm} = 60^\circ$$

We can then calculate the phase boost.

$$\phi_{boost} = -90^\circ + \phi_{pm} - \angle G_{ps}(s)_{f_c} \quad (12)$$

$$\phi_{boost} = -90^\circ + 60^\circ - 150^\circ$$

$$\phi_{boost} = -120^\circ$$

Once we have our phase boost we can calculate the phase of our controller at the crossover frequency

$$(13)$$

$$\angle G_c(s)_{f_c} = -210^\circ$$

so using the earlier equations for the magnitude and phase of the controller you can find our gains to be:

$k_i = 806.1$  and  $k_p = .444$

Once we calculated our gains we applied them to a psim simulation seen in Figure 19 to test the response of the controller.

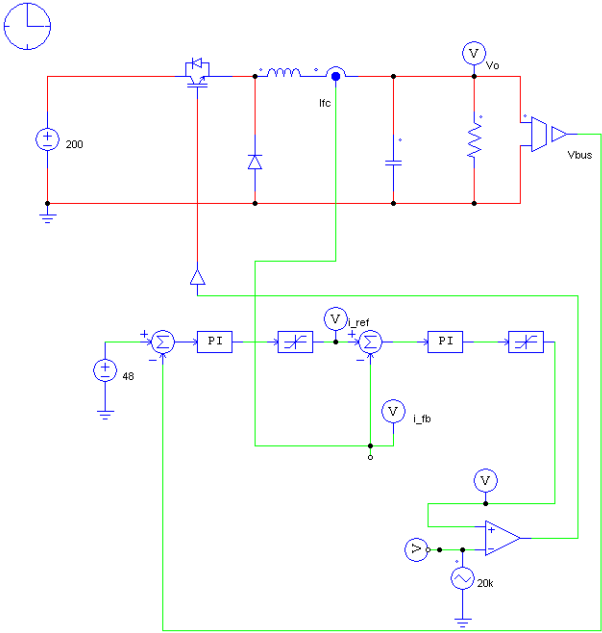


Figure 19 PSIM model of control for the buck converter

You can see in Figure 20 that the output voltage responded with little overshoot and a very fast settling time.

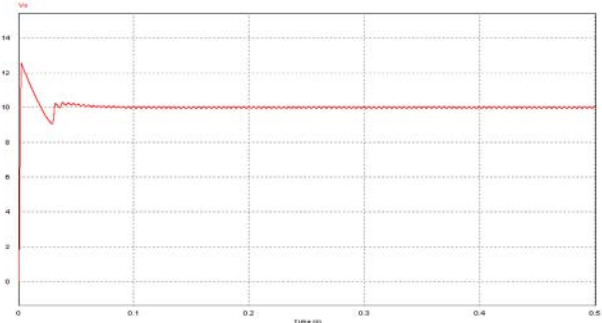


Figure 20 Output voltage response to PSIM simulation

We then built the Simulink model seen in Figure 21 to run the control for the buck converter on the DSP. When the Simulink file is compiled it generates a C code file in Code Composer and



loads it onto the DSP. When testing with the small-scale model with the input of 20V so we could expect the output to be smaller than that as a buck converter. The outputs were very accurate as seen in Figure 22.

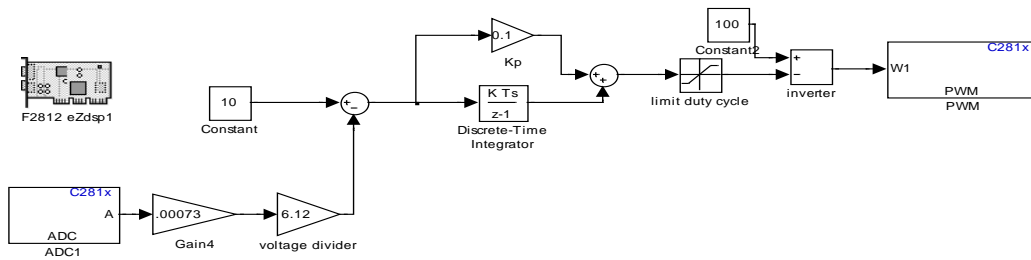


Figure 21 Simulink Control model used to generate C code for the buck converter

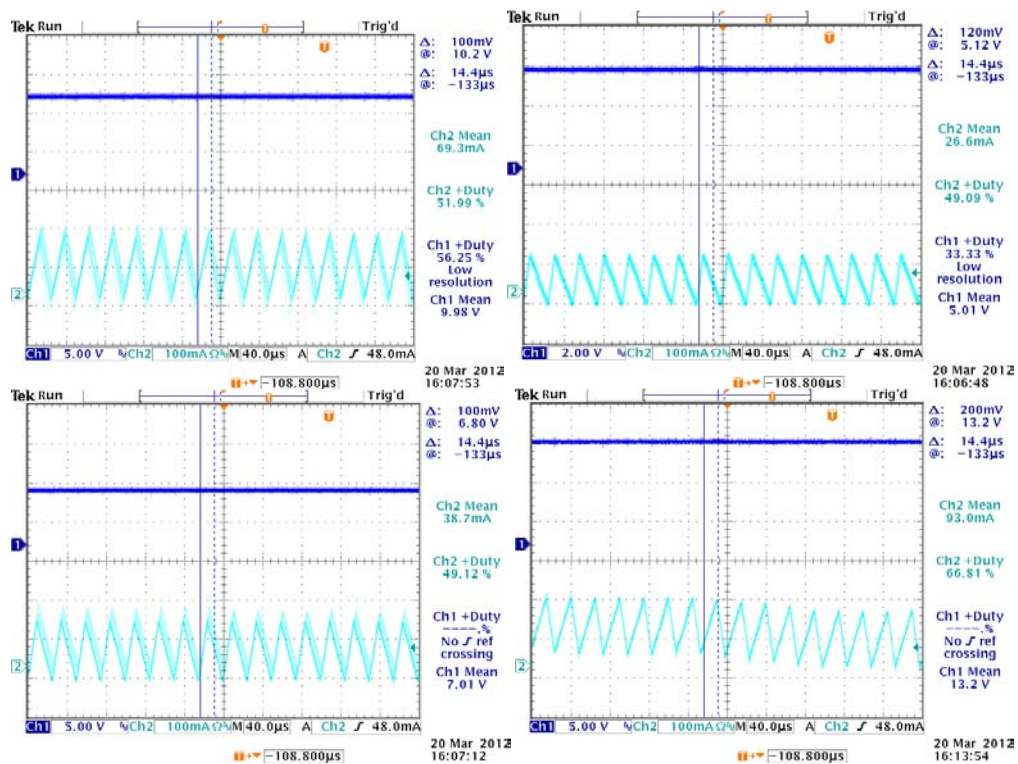


Figure 22 Channel 1 output shows the output voltage when the voltage reference is 10V, 5V, 7V and 13V.

We then used the same method described previously to calculate the  $K_p$  and  $K_i$  gains for the small-scale boost converter. After testing them in PSIM we created the Simulink model seen

in Figure 23. This again was compiled into Code Composer to generate C code for the DSP to run.

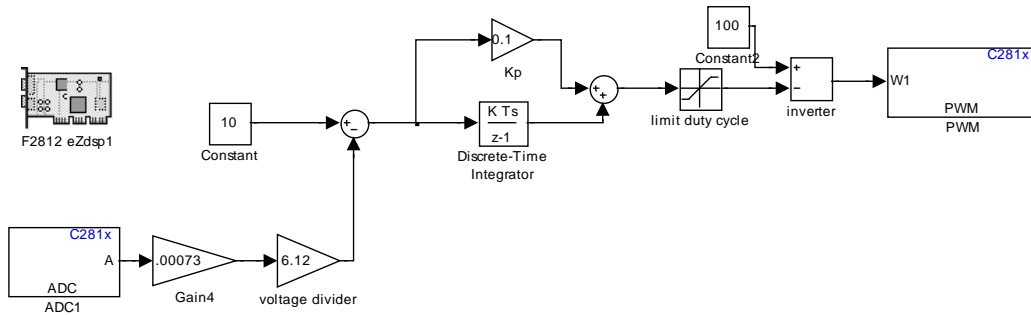
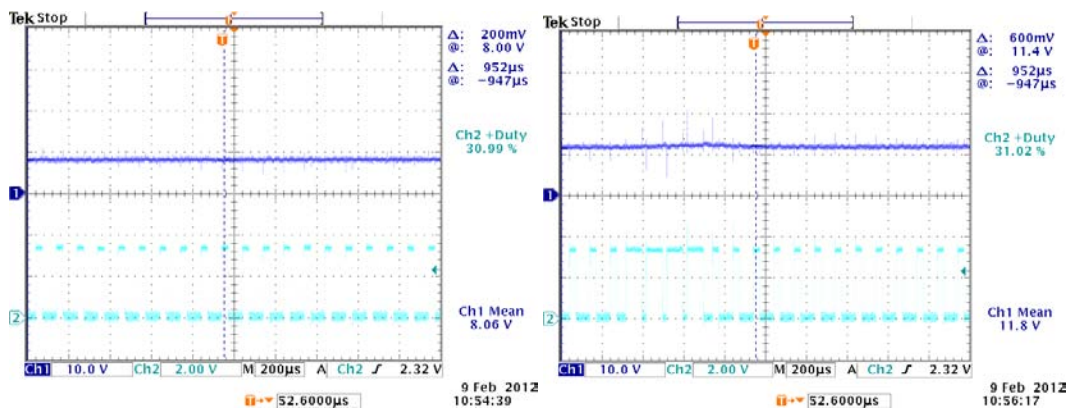


Figure 23 Boost Converter control system in Simulink

With a 5V input into our system we can expect the output to be larger than that. As seen below in Figure 24, the output voltages matched the constant reference value accurately.



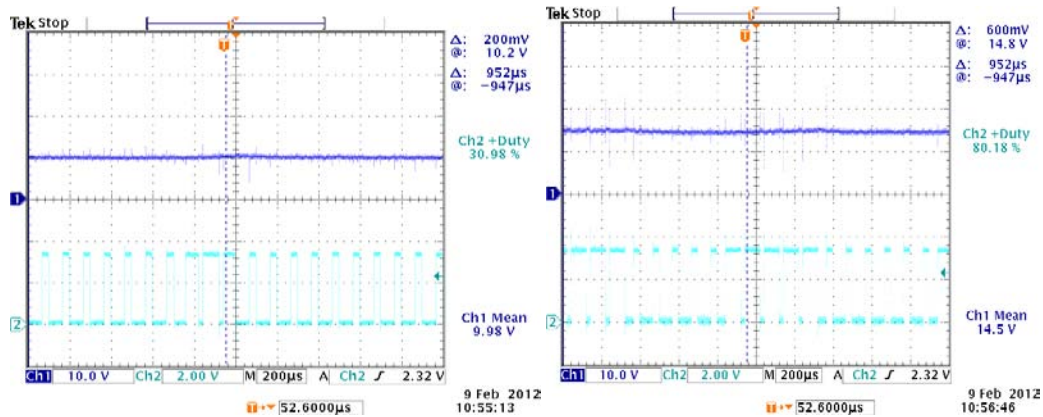


Figure 24 Results from closed loop boost converter. Channel 1 shows output voltage.

## Completed Work

Over the course of a year our team has successfully designed a full-scale system to charge and discharge a battery from wall power. We constructed small-scale circuitry to design the control systems. And from there constructed a full-scale buck converter and boost converter that successfully implemented our control system on.

## Future Work

There is much work that can be done for any interested groups in the future who wish to follow-up with this project. A future group could use the system to charge the battery. First the team would need to acquire detailed parameters for battery. The team could also implement the second stage of the system that discharges the battery through an inverter to run an AC induction motor. With this motor would come the possibility of a regenerative braking system. In order to optimally store the energy created by the regenerative braking, ultra-capacitors could be utilized for quick charging capabilities.

## IMPLEMENTATION AND SIMULATION

Prior to this year, no Bradley Electrical Engineers have worked on this design. Under the advisory of Dr. Na, we have started this project from the ground up. The information provided

ahead is a way to inform the reader about Power Electronic circuits used and how they are used on a practical level given specific design specifications through simulation and lab results.

**Experimental/Simulation Setup, Results and Discussion**

Based off of our calculations, we came up with capacitor values of 1500uF and inductor values of 500uH. These values will work for both the power factor correction boost converter as well as the bi-directional converter.

**Power factor Correction**

Below is the simulation design of our Power Factor Correction circuit.

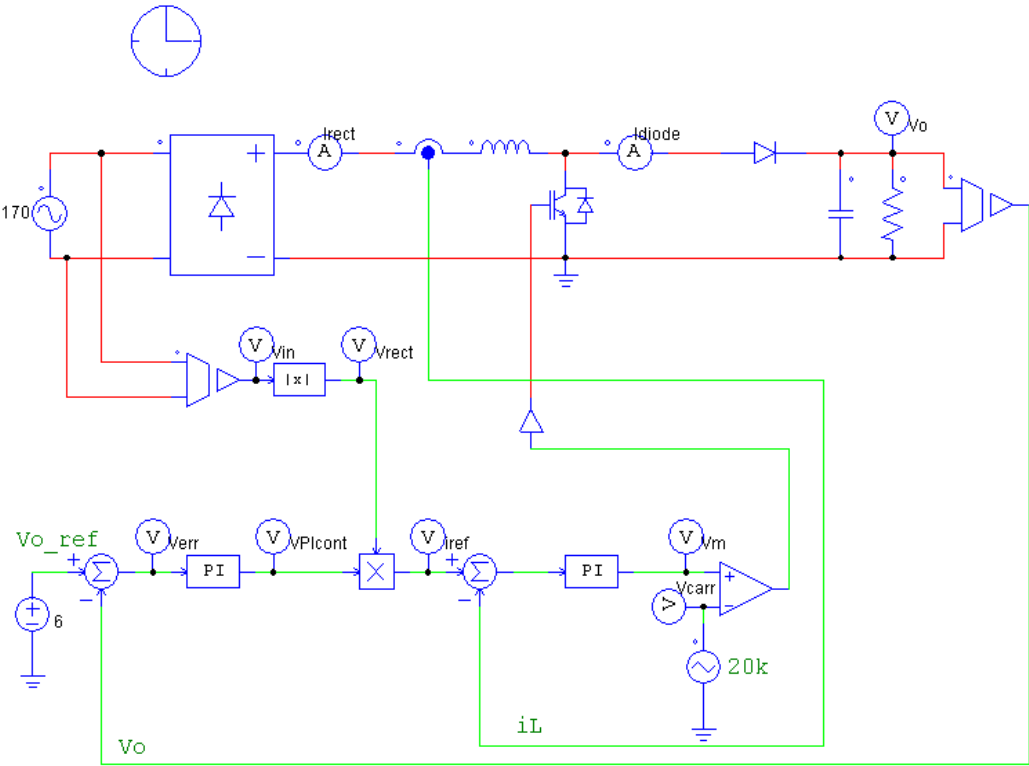


Figure 25 PSIM schematic of the power factor correction circuit (top half) and control system to be implemented on the DSP (bottom half)

Something to note is that the voltage input in the simulation is 170Vac-peak but a wall input is 120Vrms, both values are equal in some sense the 170V is a peak value while the 120V outlet is rms value . We chose to use the 170V to be aware of the max possible input into our

circuit to get the best simulation results to develop a safe circuit. After running the PSIM simulation, we acquired our desired results with the component values selected as well as a fine tuned control system. For the Power Factor Correction circuitry in Figure 25, we wanted to improve the power factor thus improving the efficiency as well as generating a DC output around 200Vdc.

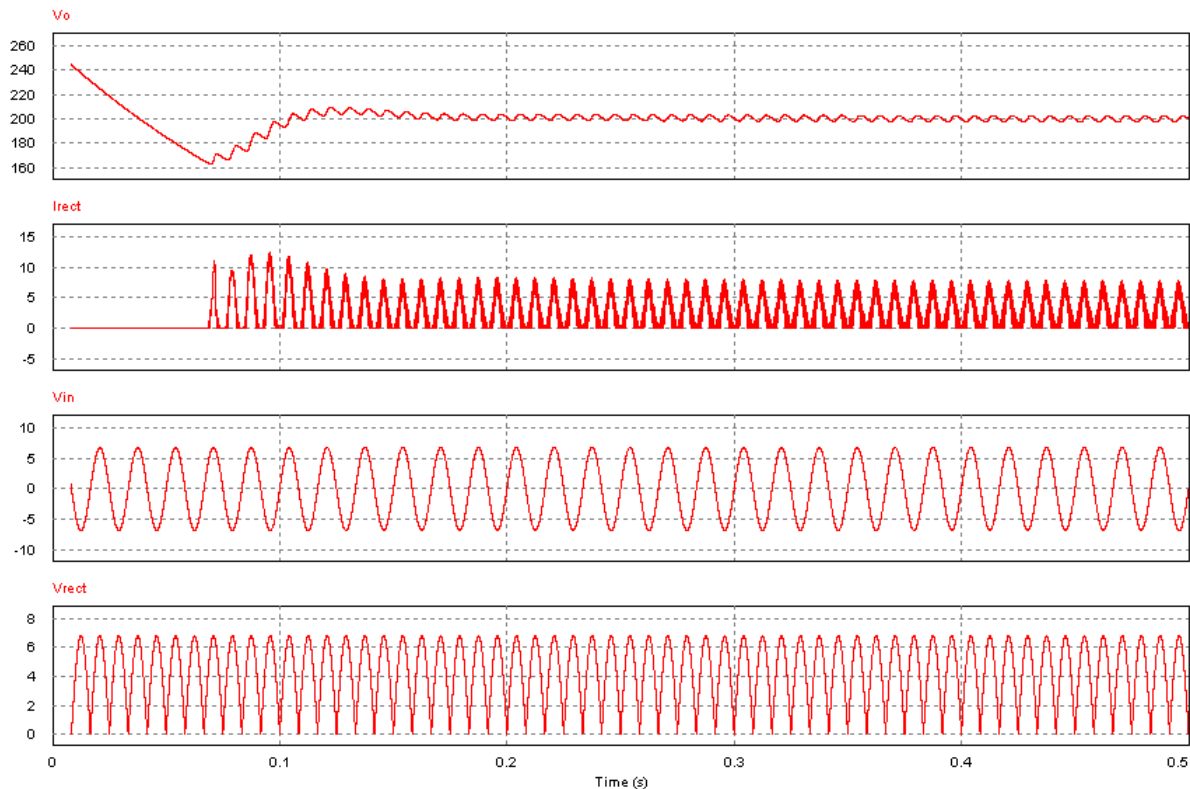


Figure 26 Simulated Output generated from the PFC boost converter and Diode Rectifier circuit.

### Bi-Directional Converter (Buck and Boost)

We chose to simulate this in two parts, the boosting stage and the bucking stage. In the final design this will only be one circuit. We designed the circuit to use a 51.8V Battery in our system. As a result we will need to lower the 200V output from the Power Factor Conversion Boost Converter to a safe 51.8V in order to charge the battery. The simulation results are shown in Figure 28.

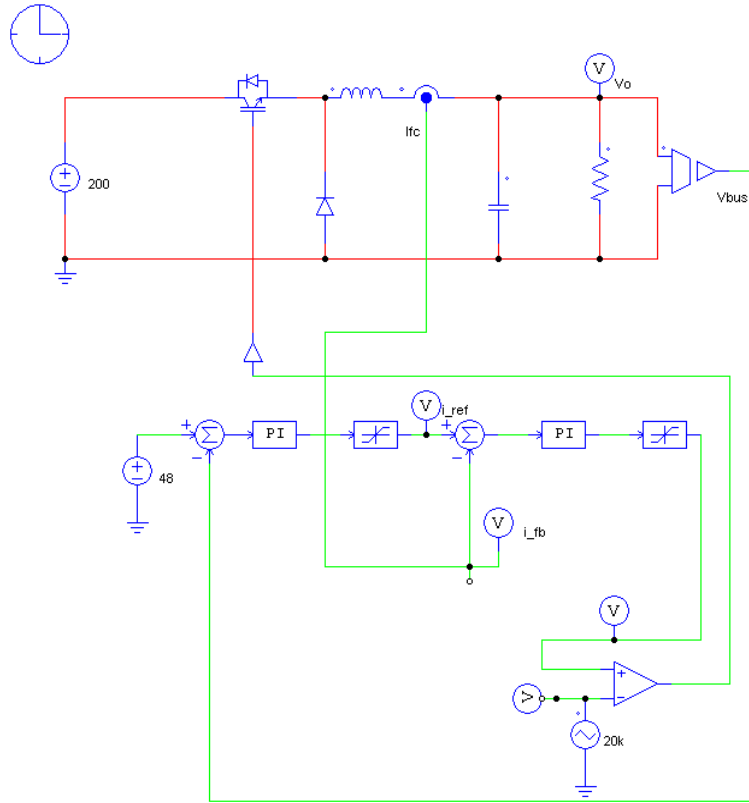


Figure 27 PSIM schematic of the bucking circuitry for the Bi-Directional Converter (left half) and control system to be implemented on the DSP (right half)

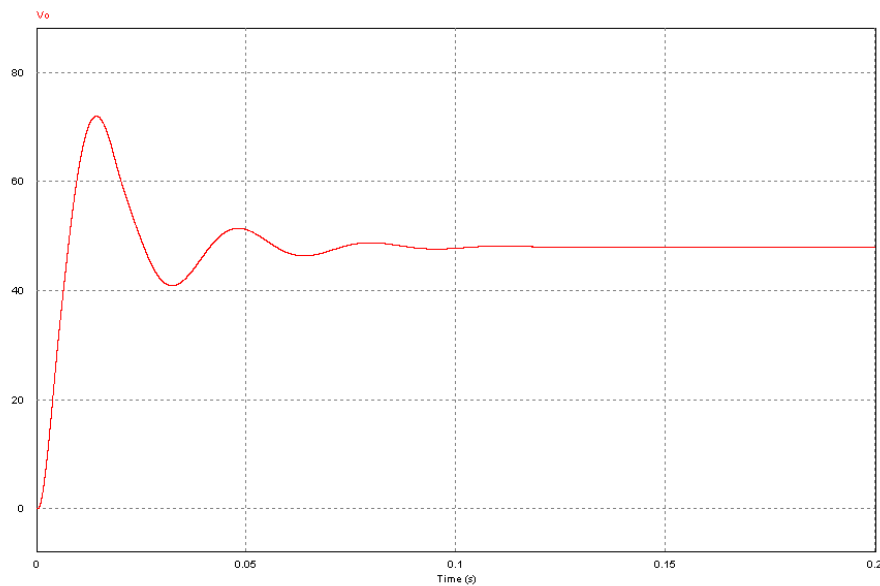


Figure 28 Output from the Bi-Directional Converter (Buck) to the 51.8V battery

The above graph is the voltage output from the buck stage of the Bi-Directional Converter. The Voltage reaches a steady state at 51.8V, which is our desired output to charge the battery. There is a good amount of initial overshoot for the first 0.05 seconds. This could be reduced by further tuning of the Proportional Integral control on the DSP.

The next stage of the Bi-Directional Converter will be the boosting stage. When the circuit is no longer charging, the battery will be responsible for discharging to the load. As part of the design specifications we need to supply 200V to the load. Currently, the battery can output 51.8V using the boost stage of the Bi-Directional converter we can achieve the 200V output. The Output results are shown in Figure 29.

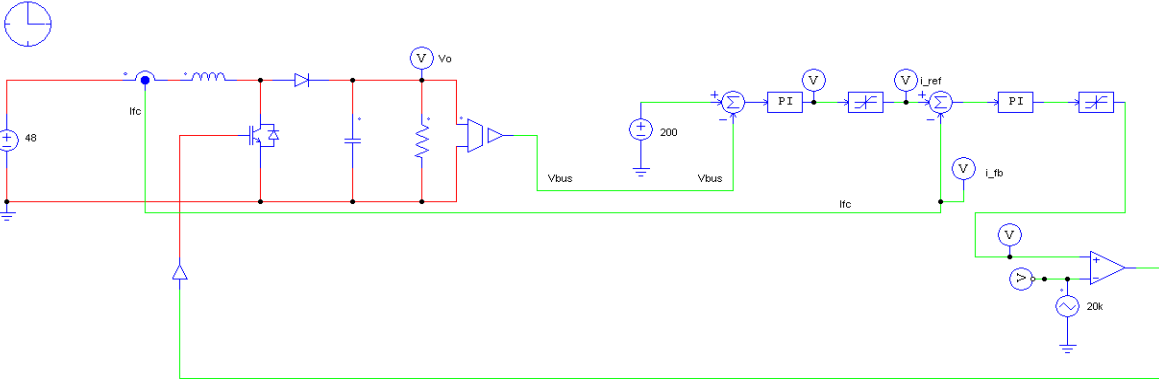


Figure 29 PSIM schematic of the boosting circuitry for the Bi-Directional Converter (left half) and control system to be implemented on the DSP (right half)

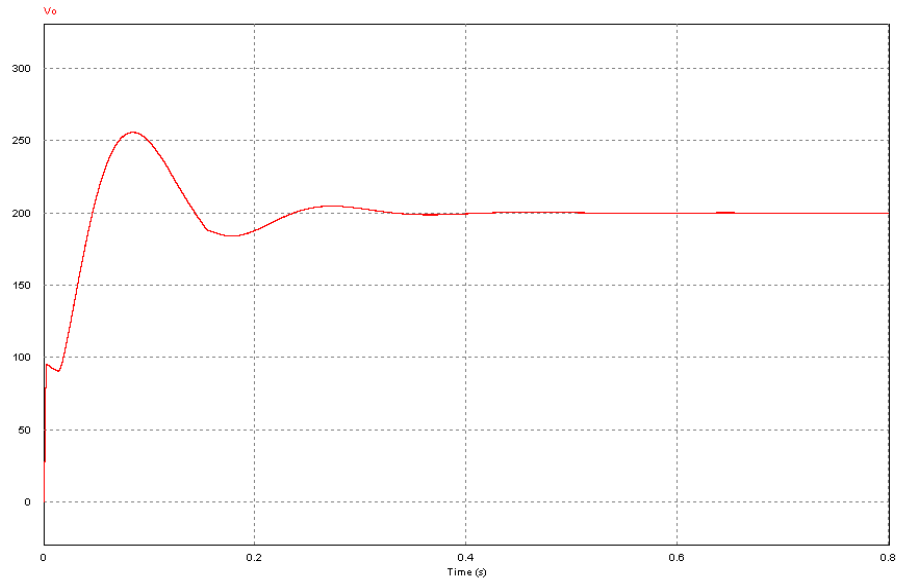


Figure 30 Output from the Bi-Directional Converter (Boost) to the 200V load

Figure 30 is the voltage output from the boost stage of the Bi-Directional Converter. The Voltage reaches a steady state at 200V. Like the buck converter, there is also some overshoot for the first 0.2 seconds. This too can be reduced by further fine tuning the PI controller via the DSP.



## Overall Schematic

In Figure 31 below is the overall schematic, showing all the connections of the entire PHEV charging system.

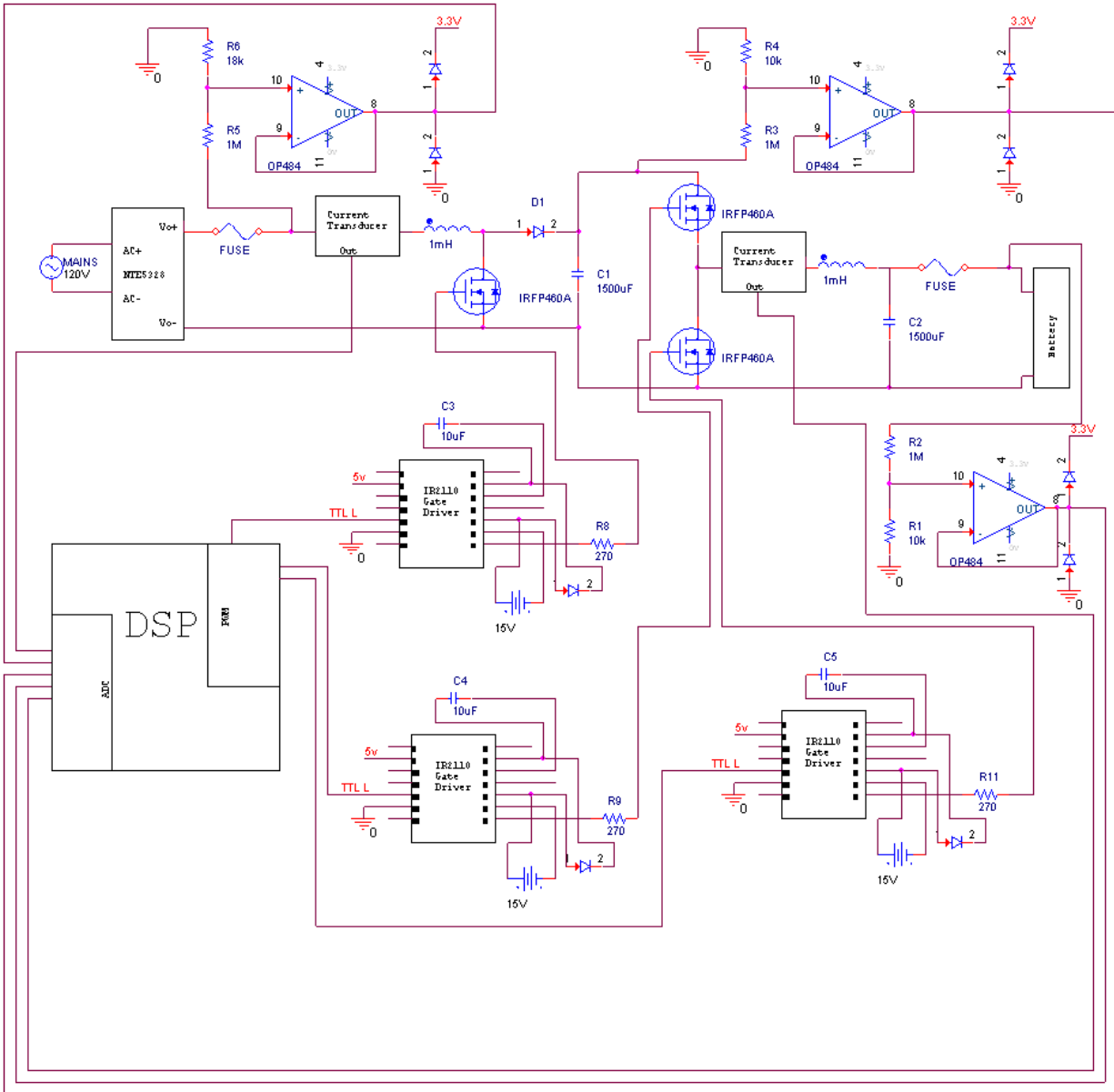


Figure 31. – Overall system schematic

## **Conclusion**

The importance of hybrid and electric vehicles is growing in today's society, due to the need to reduce our dependency on foreign oil. Developing systems like the PHEV charger to implement in vehicles is a huge step in that direction. Further research and development in the field of technology will lead to a greener future.

## References

- [1] G. Mathieu, "Design of an on-board charger for plug-in hybrid electrical vehicle (PHEV)," Master Thesis, Chalmers University of Technology, Göteborg, Sweden, 2009. apply the theory provided, run simulations and design a control system. The amount of detail in this thesis helps clarify some of the difficult hurdles of the overall project.
- [2] N. Mohan, *First Course on Power Electronics*. Minneapolis: MNPERE, 2009.
- [3] Y. Lee. A. Khaligh. and A. Emandi. (2009). Advanced integrated bidirectional AC/DC and DC/DC converter for plug-in hybrid electric vehicles. *IEEE Transactions on Vehicular Technology*. [Online]. 58 (8), pp. 3970-3980. Available: <http://ieeexplore.ieee.org.ezproxy.bradley.edu/stamp/stamp.jsp?tp=&arnumber=5170004>
- [4] B. Bagci, "Programming and use of TMS320F28I2 DSP to control and regulate power electronic converters," Master Thesis, Fachhochschule Koln University of Applied Sciences, Cologne, Germany, 2003.
- [5] [http://batteryuniversity.com/learn/article/charging\\_lithium\\_ion\\_batteries](http://batteryuniversity.com/learn/article/charging_lithium_ion_batteries)
- [6] <http://www.nrel.gov/docs/fy01osti/28716.pdf>
- [7] <http://www.irf.com/technical-info/appnotes/an-978.pdf>

## Sources Consulted

- D. M. Bellur and M. K. Kazimierczuk. (2007). DC-DC converters for electric vehicle applications. *Electrical Insulation Conference and Electrical Manufacturing Expo*. [Online]. pp. 286-293. Available: <http://ieeexplore.ieee.org.ezproxy.bradley.edu/stamp/stamp.jsp?tp=&arnumber=4562633>
- L. Zhou, "Evaluation and DSP based implementation of PWM approaches for single-phased DC-AC converters," Master Thesis, Florida State University, Tallahassee, Florida, United States 2005.
- L. Zhu. (2004). A novel soft-commutating isolated boost full-bridge ZVS-PWM DC-DC converter for bidirectional high power applications. *Power Electronics Specialists Conference*. [Online]. 3, pp. 2141-2146. Available: <http://ieeexplore.ieee.org.ezproxy.bradley.edu/stamp/stamp.jsp?tp=&arnumber=1355450>
- M. Hedlund, "Design and construction of a bidirectional DCDC converter for an EV application," Master Thesis, Uppsala University, Uppsala, Sweden, 2010.
- M. Marchesoni. (2007). New DC-DC converter for energy storage system interfacing in fuel cell hybrid electric vehicles. *IEEE Transactions on Power Electronics*. [Online]. 22 (1), pp. 301-308. Available: <http://ieeexplore.ieee.org.ezproxy.bradley.edu/stamp/stamp.jsp?tp=&arnumber=4052425>
- Y. Tian, "Analysis, simulation and DSP based implementation of asymmetric three-level single-phase inverter in solar power system," Master Thesis, Florida State University, Tallahassee, Florida, United States, 2007.

## Appendix A

```
clear all
close all
```

```
num = [29971 4.3e8];
den = [1 1.3587e3 1.4347e7]; % voltage mode control Fig-4-18
```

```
figure(1)
% f = linspace(30,30e3,500); % generate frequency points to be evaluated
f = logspace(1,4,500); % generate frequency points in log scale
w = 2*pi*f; % 'freqs' needs frequency in radians/sec
H = freqs(num, den, w) % to obtain frequency responses: amplitude and phase
amp = abs(H); % amp in linear scale
phase = angle(H)*180/pi;
```

```
magdB = 20*log10(amp); % magdB is the amplitude frequency response in decibel.
```

```
figure(1), subplot(211), semilogx(f, magdB(1,:)), title('amplitude response in dB'),grid
subplot(212),semilogx(f, phase(1,:)), title('phase response in degree')
grid, xlabel('frequency in Hz'),ylabel('degree')
```

## Appendix B

### Materials/Parts List

- IRFP460A N-Type Power MOSFET
  - SK 145 Heat Sink
- IR2110 - 1PBF MOSFET Driver
- NTE5328 – Bridge Rectifier
- VS-HFA50PA60CPBF Power Diode
- L08P050D15 Current Transducer
- OP484FPZ Op-Amp
- NXP - 74HC04N Hex Inverter
- Aluminum Electrolytic Capacitor 1500uF, 400V
- Inductor 500uH, 35A
- Resistors & Power Resistors (Assorted Values)
- 51.8V Li-ion Battery
- Oscilloscope
- DC Power Supply Unit
- Signal Generator
- DSP
  - TMS320F2812 DSP
  - Code Composer Studio 3
  - Mathworks Matlab & Simulink
- Psim Software